

Unconventional Superconductivity Induced by Quantum Critical Fluctuations in
Hydrate Cobaltate $\text{Na}_x(\text{H}_3\text{O})_z\text{CoO}_x \cdot y\text{H}_2\text{O}$

| Relationship between Magnetic Fluctuations and the Superconductivity Revealed
by a Co Nuclear Quadrupole Resonance |

Y. Ihara,¹ H. Takeya,¹ K. Ishida,¹^y H. Ikeda,¹ C. M. Ichioka,² K. YOSHIMURA,² K. Takada,³ T. Sasaki,³
H. Sakurai⁴ and E. Takayama-Muromachi⁴

¹ Department of Physics, Graduate School of Science, Kyoto University, Kyoto 606-8502, Japan,

² Department of Chemistry, Graduate School of Science, Kyoto University, Kyoto 606-8502, Japan

³ Nanoscale Materials Center, National Institute for Materials Science, Tsurukawa, Ibaraki, 305-0044, Japan

⁴ Advanced Nano Materials Laboratory, National Institute for Materials Science, Tsurukawa, Ibaraki 305-0044, Japan.

A Co nuclear-quadrupole-resonance (NQR) measurement was performed on various bilayered hydrate $\text{Na}_x(\text{H}_3\text{O})_z\text{CoO}_x \cdot y\text{H}_2\text{O}$ with different values of the superconducting and magnetic-ordering temperatures, T_c and T_M . From measurements of the temperature and sample dependence of the NQR frequency, it was revealed that the NQR frequency is changed due to the change of the electric field gradient (EFG) along the c axis $_{zz}$ rather than the asymmetry of EFG within the ab-plane. In addition, it is considered that the change of $_{zz}$ is determined mainly by the trigonal distortion of the CoO_2 block layers along the c axis from the relationships between $_{zz}$ and the various physical parameters. We found a tendency that the samples with $_{zz}$ larger than 4.2 MHz show magnetic ordering, whereas the samples with lower $_{zz}$ show the superconductivity. We measured nuclear spin-lattice relaxation rate $1/T_1$ in these samples, and found that the magnetic fluctuations depend on sample. The higher- T_c sample has a stronger magnetic fluctuations at T_c . From the relationship between $_{zz}$ and T_c or T_M , we suggest that the NQR frequency is regarded as a tuning parameter to determine the ground state of the system, and develop the phase diagram using the $_{zz}$. The phase diagram we developed shows that the highest- T_c sample is located at the point where T_M is considered to be zero, and suggests that the superconductivity is induced by the quantum critical fluctuations. We strongly suggest that the hydrate cobaltate superconductor is an example of magnetic-fluctuation-mediated superconductivity argued in the heavy-fermion compounds. The coexistence of the superconductivity and magnetism observed in the sample with the highest $_{zz}$ is also discussed on the basis of our experiments.

KEY WORDS: superconductivity, hydrous sodium cobalt oxide, NQR, spin fluctuations

1. Introduction

Since the superconductivity in hydrate cobaltate $\text{Na}_{0.3}\text{CoO}_2 \cdot 1.3\text{H}_2\text{O}$ was discovered,¹ a lot of studies have been done from both experimental and theoretical points of view. The superconductivity on the two dimensional CoO_2 layer with triangular lattice is attractive from the comparison with the cuprate and ruthenate compounds, in which superconductivity occurs in the square lattices. In the cobaltate compounds, the superconductivity emerges only when water molecules are sufficiently intercalated between the CoO_2 layers. This superconducting structure is called as bilayered hydrate (BLH) structure, in which the double water layers sandwich a Na layer and the water-Na block layer is formed.² The BLH compounds are quite unstable and the sample quality are easily degraded under an ambient condition, since water molecules easily evaporate into the air.³ After the evaporation of some water, the BLH structure changes to a single-layer structure, in which the water-Na block layer is changed to a single water-Na layer.⁴ This is called as monolayered hydrate (MLH) structure

and does not show any superconductivity. It is considered that the water intercalation plays an important role for the occurrence of the superconductivity. Several roles of the water intercalation are already pointed out as follows. First, two dimensionality is enhanced by the water intercalation, since the c-axis lattice parameter in the BLH compound is almost twice as that of non-hydrated Na_xCoO_2 .⁵ As a result, the interlayer coupling observed in the non-hydrated compounds found by neutron scattering measurement^{6,7} is suppressed by the water intercalation.⁵ Second, the random occupation of the Na^+ ions is screened by the double water layers. Actually, single Co nuclear quadrupole resonance (NQR) peak is observed in the BLH compound, whereas two peaks with a satellite structure are observed in the MLH compound. The NQR results indicate that the electric field gradient (EFG) at the Co sites in the CoO_2 layer is unique in the BLH compound but the several Co EFG sites are present in the MLH compound.⁸ Third, the compression of the CoO_2 block layers along the c axis is induced by the water intercalation.⁹ When the c-axis lattice parameter is elongated by the water intercalation, the coupling between the positive Na^+ and the negative oxygen O^{2-}

E-mail address: ihara@scphys.kyoto-u.ac.jp

^yE-mail address: kishida@scphys.kyoto-u.ac.jp

ions becomes weaker. As a result, the oxygen ions shift toward the positive Co ions, resulting in the squeeze of the CoO_2 block layers. The neutron diffraction measurements show that T_c increases with decreasing the CoO_2 layer thickness.¹³ Although water content is regarded as an important factor for the superconductivity, it is difficult to control the content precisely due to the soft chemical procedure.¹⁴ This is the reason why there exists a large sample dependence in this system.

Other controversial issue is the Fermi-surface (FS) properties in the cobaltate compounds. The LDA band calculation in NaCo_2O_4 done by Singh suggested that the FS's of the compound consist of a large hole-like FS composed of a_{1g} -orbital around the Γ point and six small hole pockets composed by e_g^0 -orbitals around the K points.¹⁵ However, angle-resolve photoemission spectroscopy (ARPES) experiments done by several groups revealed the large a_{1g} -like FS and the absence of the small hole pockets, and found that the e_g^0 bands and the associated small pockets sink below the Fermi energy,¹⁶⁻¹⁸ although the bands and the pockets are reported to be lifted by the water-intercalation. The topology of the FS's in the hydrate and anhydrate cobaltate is still uncertain at present, but is quite important for developing the theoretical scenario for occurrence of the unconventional superconductivity.²⁰⁻²² We point out that the investigation of the magnetic fluctuations in anhydrate, MLH and BLH compounds gives important information about the FS in these compounds, because the magnetic fluctuations are induced by the nesting of the FS's.

We have performed Co-NQR measurements on various samples with different superconducting and magnetic ordering temperatures T_c and T_M in order to investigate sample dependence of the magnetic fluctuations in the superconducting cobaltate and to find the key factors for occurrence of the superconductivity. We found that the NQR frequency ω and the magnetic fluctuations strongly depend on sample. After the investigation of the relationship between the observed ω and various physical parameters, it was found that ω is scaled to the c-axis lattice parameter and is related with T_c . In addition, the samples with higher ω show a magnetic ordering. We consider that ω is one of the important physical quantities to determine the electronic state and develop the phase diagram of the cobaltate superconductor using ω . The phase diagram we show here indicates that the highest- T_c sample is situated at the point where magnetic-ordering temperature becomes zero, and suggests that the superconductivity on the BLH cobaltates is induced by the quantum critical fluctuations.

2. Experiment

We used twelve samples, which were synthesized as described in literatures.^{4,14} The crystalline parameters and Na content x are precisely measured by X-ray diffraction and inductively-coupled plasma atomic emission spectroscopy (ICP-AES), respectively and the Co valence v in several samples are measured by redox titration measurements. The superconducting transition temperature T_c is determined from the onset of the superconducting

demagnetism. The NQR spectra are obtained by recording signal intensity with changing the frequency. Various physical parameters are listed in table I. From the redox-titration measurements, it was already pointed out by several groups that the valence of Co v cannot be interpreted by the chemical formula of $\text{Na}_x\text{CoO}_2 \cdot y\text{H}_2\text{O}$, since the Na content x is not equal to be 4 v .²³ Taking into account the presence of oxonium ion H_3O^+ , it becomes widely accepted that the chemical formula is expressed as $\text{Na}_x(\text{H}_3\text{O})_z\text{CoO}_2 \cdot y\text{H}_2\text{O}$.²⁴ Here, the oxonium content is determined to be $z = 4 - x$. Nuclear spin-lattice relaxation rate $1/T_1$ was measured at a maximum peak of the NQR signal arising from a $5=2 \leftrightarrow 7=2$ transition in each sample. The recovery of the nuclear magnetization after saturation pulses can be fitted by the theoretical curves in whole temperature range. To get reliable data and keep the sample quality during the measurement, all samples are preserved in the freezer or in liquid N_2 , and thus the superconducting and magnetic transition temperatures and NQR results in each sample are reproduced during the experiments.

Table I. Na content, c axis length, transition temperature, Co valence and NQR frequency arising from the transition between $5=2 \leftrightarrow 7=2$.

No.	Na content	c (Å)	T_c (K)	Co^{+v}	ω (MHz)	ref.
1	0.346	19.684	4.7		12.30	8
2	0.339	19.720	4.6		12.30	10
3	0.348	19.569	2.8		12.07	9
4	0.35	19.603	4.6		12.32	9
5	0.331	19.751	0.0	3.42	12.54	9
6	0.351	19.714	4.6	3.37	12.45	11,12
7	0.350	19.739	4.4	3.41	12.50	
8	0.322	19.820	3.6	3.40	12.69	
9			3.6		12.22	
10	0.38	19.588	2.6	3.49	12.10	
11	0.358	19.614	3.5	3.47	12.18	
12	0.346	19.691	4.8	3.48	12.39	

3. Experimental results

3.1 NQR spectrum

The nuclear Hamiltonian with the nuclear electric quadrupole (eqQ) interaction is described as

$$H_Q = \frac{zz}{6} 3I_z^2 - I^2 + \frac{(I_+^2 + I_-^2)}{2}$$

, where quadrupole frequency zz is defined as $3e^2qQ=2I(2I-1)$ with the electric field gradient (EFG) along the z axis, $eq = V_{zz}$ and the nuclear quadrupole moment Q , and z is the asymmetry parameter of EFG expressed as $(V_{xx} - V_{yy})/V_{zz}$ with V which is EFG along direction ($= x; y; z$). The nuclear spin of Co is $I = 7=2$, and three NQR peaks are observed from $1=2 \leftrightarrow 3=2$, $3=2 \leftrightarrow 5=2$, and $5=2 \leftrightarrow 7=2$ transitions, respectively. The typical NQR spectrum in a superconducting cobaltate is shown in Fig. 1. Because of the existence of asymmetry of EFG in the ab plane, the separation between two peaks is not the same. Within the second order perturbation against the asymmetry

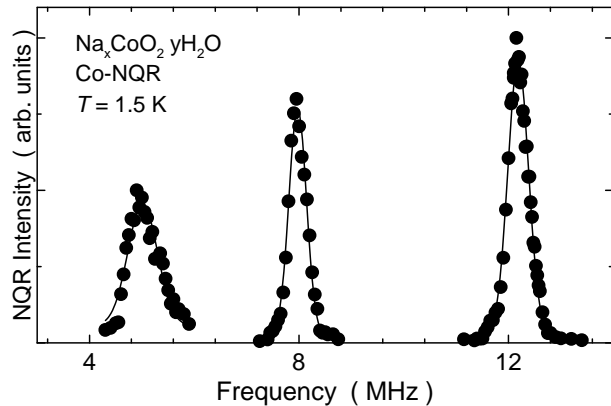


Fig. 1. Co-NQR spectra at 1.5 K in the sample No. 11. These peaks originate from three transitions. From these peak frequencies, ω_0 and ω_1 are evaluated to be 4.08 MHz and 0.20, respectively.

parameter in the ab plane, resonance frequencies are described as,

$$\omega_1 = \omega_{zz} 1 + \frac{109}{30} \omega_2^2 \quad (\text{for } 1=2 \text{ and } 3=2);$$

$$\omega_2 = 2 \omega_{zz} 1 - \frac{17}{30} \omega_3^2 \quad (\text{for } 3=2 \text{ and } 5=2);$$

$$\omega_3 = 3 \omega_{zz} 1 - \frac{1}{10} \omega_2^2 \quad (\text{for } 5=2 \text{ and } 7=2);$$

Both ω_{zz} and ω_1 are obtained by solving above equations. ω_{zz} is determined by several factors such as the Co valence, the hole density of the Co 3d orbitals and the crystal structure, particularly the distance between O^{2-} and Co^{3+} ions.

In order to investigate temperature dependence of ω_{zz} and ω_1 , both of ω_2 and ω_3 are measured up to 150 K in the No. 11 sample shown in Fig. 1. As seen in Fig. 2 (a), both ω_2 and ω_3 are nearly constant below 50 K, and shift toward a lower frequency with increasing temperature. Temperature dependences of ω_{zz} and ω_1 , which are derived from the temperature variation of ω_2 and ω_3 , are shown in Fig. 2 (b). We found that the temperature dependence of ω_{zz} is similar to that of the c-axis lattice parameter measured by the neutron diffraction,¹³ and suggest that temperature dependence of ω_{zz} is mainly determined by that of the c-axis parameter.¹³ In contrast to the considerably large temperature dependence of ω_{zz} , ω_1 is unchanged with temperature and is estimated to be 0.2. Since ω_1 originates from the anisotropy of EFG along x and y directions, it should be noted that ω_1 is zero in a perfect triangular lattice. The finite value of ω_1 suggests some distortions are present in the x-y direction of the CoO_2 layer. The possible origin of ω_1 will be discussed in section 4.1.

Figure 3 shows the NQR spectra arising from the 5=2 and 7=2 transition in various samples with different contents of H_2O , Na^+ and H_3O^+ . ω_{zz} and ω_1 are evaluated in these samples. The ratio of ω_3 and ω_2 , ω_3/ω_2 (R) is plotted against ω_3 in Fig. 4 (a). The ratio R is R = (18 - 9=5^2) = (12 - 34=5^2). This value depends

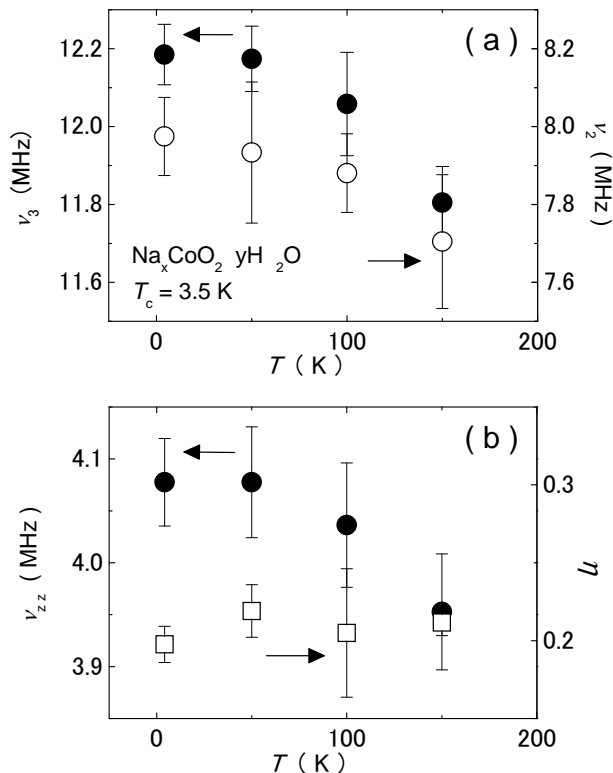


Fig. 2. (a) Temperature dependence of ω_3 and ω_2 measured on the No. 11 sample. (b) Temperature dependence of ω_{zz} and ω_1 , which are evaluated from ω_2 and ω_3 in (a).

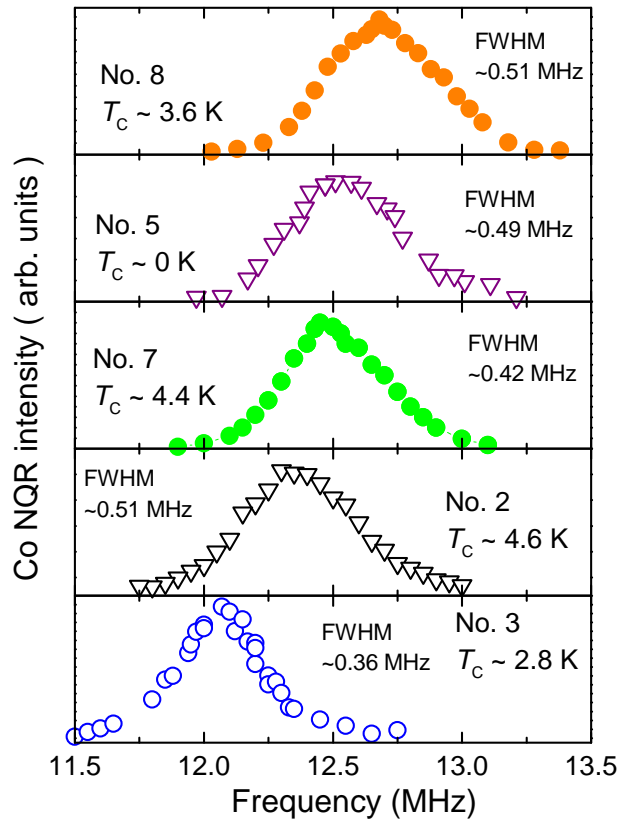


Fig. 3. Co-NQR spectra arising from the 5=2 and 7=2 transition in various samples measured at 4.2 K. In magnetically ordered samples (No. 5 and No. 8), the spectra were measured at 8 K above ordered temperatures. T_c and the full width at half maximum in each sample are shown.

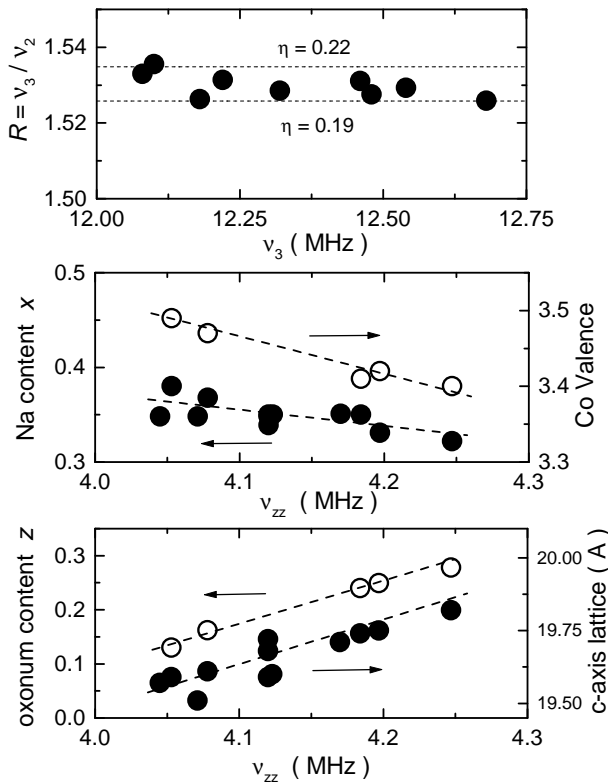


Fig. 4. (a): $R = v_3/v_2$, which is related to v_3 , is plotted against v_3 . (b) and (c): various physical parameters (Na content x , Co valence v , oxonium content: z , and c-axis lattice parameter) are plotted against v_{zz} .

solely on v_{zz} and is free from v_{zz} . The values of R are within the values expected when $0.19 < \eta < 0.22$ as seen in Fig. 4 (a), and are nearly independent of the sample. This indicates that the sample dependence of NQR frequency originates mainly from v_{zz} . Similar to the result of the temperature dependence, v_{zz} is almost unchanged within these samples although Na^+ and H_3O^+ contents would be different in these samples. v_{zz} is plotted against various physical parameters such as Na content x and Co valence v (Fig. 4 (b)), the oxonium content z , and the c-axis parameter (Fig. 4 (c)), where the oxonium content z is estimated from the relation of $z = 4 - x - v$. Detailed discussion about the electric field gradient will be done in the section 4.1.

3.2 Nuclear spin-lattice relaxation rate

Figure 5 shows temperature dependence of $1/T_1T$ in various BLH samples below 200 K together with that in a MLH sample, which does not show superconductivity down to 1.5 K. The values of $1/T_1T$ in all samples show the similar temperature dependence down to 70 K, which is characterized as a weak pseudogap behavior. Below 70 K, $1/T_1T$ shows sample dependence. The non-superconducting MLH sample shows the Korringa behavior down to 1.5 K, indicative of the absence of temperature-dependent magnetic fluctuations. Whereas the values of $1/T_1T$ in superconducting samples increase with decreasing temperature below 70 K down to T_c , and the values of $1/T_1T$ at T_c is larger in the higher- T_c sample. Similar tendency of $1/T_1T$ in various superconduct-

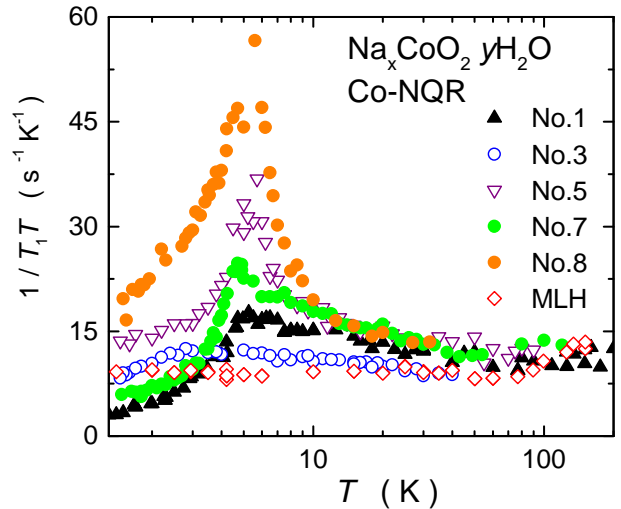


Fig. 5. Temperature dependence of $1/T_1T$ in various samples. The values of $1/T_1T$ at T_c (or just above T_N) increase as the NQR frequency is higher.

ing samples was reported by Zheng et al.²⁵ In magnetic samples (No. 5 and 8), $1/T_1T$ shows a prominent peak at T_M , below which an internal field appears at the Co nuclear site. The ordered moment in the No. 5 sample was estimated to be approximately the order of 0.01 μ_B using the observed internal field strength and the hyperfine coupling constant at the Co site.⁹ It is noteworthy that the temperature dependence of $1/T_1T$ in the high- T_c sample (No. 1) is the same as that in the magnetic sample in the temperature range of 15 – 100 K. This suggests that the high- T_c samples have similar magnetic fluctuations as the magnetic ordering samples. In addition, the low- T_c sample (No. 3) shows a weak enhancement of $1/T_1T$ at T_c , followed by the moderate decrease of $1/T_1T$ below T_c , although the full width at half maximum (FWHM) of the NQR peak is the narrowest within all the samples. These results suggest that the origin of lower T_c is not due to the suppression of the superconductivity by the inhomogeneity and/or randomness of the sample, but due to the weakness of the pairing interaction. If T_c were suppressed by the inhomogeneity, the FWHM should be broader than the higher- T_c sample. Taking these experimental results into account, we suggest strongly that the magnetic fluctuations, which are close to magnetic instability, play an important role in the superconductivity in the BLH cobaltate. We also point out from the comparison between Fig. 3 and Fig. 5 that $1/T_1T$ below 70 K is enhanced more significantly as the NQR frequency is higher, and that there is a relationship between low-temperature magnetic fluctuations and the NQR frequency. The detailed characteristics of the magnetic fluctuations and the possible interpretation for the relationship are discussed in the section 4.2, 4.3.

We found the coexistence of magnetic ordering and superconductivity in the No. 8 sample, which has a highest NQR frequency ($v_3 = 12.69$ MHz). The magnetic ordering is identified by the prominent peak of $1/T_1T$, and the occurrence of the superconductivity is by the superconducting diamagnetic signal. The coexistence observed in

the No. 8 sample will be also discussed in the section 4.5.

4. Discussion

4.1 Analyses of EFG at the Co site

As shown in Fig. 3, the EFG at the Co site depends on sample. Here, we discuss the origin of the sample dependence of the EFG. In general, there are two sources of the EFG. One is EFG coming from the point charges on the lattice ions surrounding the Co site, V_{lat} , and the other is the intra-site effect V_{int} produced by the on-site Co-3d electrons. As shown in Fig. 4 (c), it is obvious that there exists some relationship between z_{zz} and the c-axis lattice parameter. It was reported that the c-axis lattice parameter is increased when the water molecules are inserted and/or the oxonium ions with the larger ionic radius are replaced by the Na ions. In both cases, the block layer consisting of Na/H₃O and H₂O elongates along the c axis and pushes the CoO₂ layer, so that the CoO₂ block layers are compressed in the samples with the longer c-axis. It was pointed out that the thickness of the CoO₂ block layer in the BLH compounds with the large v value is thinner than that of the MLH compounds. According to the point charge calculations, it is shown that V_{lat} is increased as the CoO₂ block is compressed along the c axis. The relationship between z_{zz} and the c-axis lattice parameter is explained consistently in this way.

Next, we discuss the contributions from the on-site 3d holes. In the cuprate superconductors, it was pointed out that the NQR frequencies at the Cu and O sites are determined by the on-site holes,²⁶ and Zheng et al. estimated the local hole content from the analyses of z_{zz} in these sites.²⁹ We introduce their analyses to the cobaltate and evaluate the hole number at the Co-3d in the superconducting cobaltate superconductor.

When we take a_{1g} and doublet e_g^0 orbitals in the trigonal structure, we describe the wave function of Co-3d orbitals which consist of the linear combination of these orbitals as

$$3d = \frac{p}{1 - w^2} |a_{1g}\rangle + \frac{w}{2} |e_g^0+\rangle + \frac{w}{2} |e_g^0-\rangle :$$

Here, w^2 is the occupation of the e_g^0 orbitals. The EFG V_z arising from the on-site holes is calculated as

$$V_z = e \frac{Z}{3d} \frac{q^2}{\theta} \frac{1}{r} \quad 3d \quad (z = x, y \text{ and } z):$$

Therefore, each component of V_z at the Co site is expressed as

$$z = n_{3d} \cdot 3d \cdot g(w);$$

where $n_{3d} = n_{a_{1g}} + n_{e_g^0}$ is the hole number in the Co-3d t_{2g} orbitals and $g(w)$ denotes the solutions of the secular equation with respect to V_z . The largest value of the solution of $g(w)$ gives the value of z_{zz} , and the smallest one gives z_{yy} . When there is one hole in the a_{1g} orbital ($w = 0$), $z_{3d,0}$ is expressed as

$$z_{3d,0} = \frac{1}{14} \frac{e^2}{h} \frac{59}{4} \frac{1}{4} \frac{4}{7} \text{hr}^3 i_{3d}$$

and is estimated that $z_{3d,0} = 20.4$ MHz and z_{yy} is zero. Here the average of r^3 for the 3d-orbitals is taken to

be $\text{hr}^3 i_{3d} = 6.7$ a.u. and the reduction factor $= 0.8$ is adopted.^{27,28}

For simplicity, if we neglect V_{lat} related to the ions surrounding the Co, and assume that the observed z_{zz} is determined solely by the on-site Co-3d hole, $w^2 = 0.25$ and $n_{3d} = 0.31$ are derived from the experimental values of $z_{zz} = 0.2$ and $z_{yy} = 4.1$ MHz. These values imply that the ratio between $n_{a_{1g}}$ and $n_{e_g^0}$ is approximately 3 : 1, and the valence of Co is +3.31, which is not so far from the directly measured v ($v = 3.45$). We point out that the non-negligible z_{yy} is not solely due to the Na-ordering effect and/or the distortion of the x-y plane, but due to the presence of holes in the e_g^0 orbitals in some degree, because z_{yy} is zero when no hole is in the e_g^0 orbitals. In addition, if we proceed this analysis at the O site in the CoO₂ layer, the hole content at the O_{2p} orbitals, which are coupled with the Co-3d e_g^0 orbitals, is evaluated to be $n_{2p} = 0.05$. This is estimated from the O-NMR value ($z_{zz} = 0.168$ MHz) and $z_{2p,0} = 3.65$ MHz with $\text{hr}^3 i_{2p} = 4.97$ a.u. by using a relation of $n_{2p} = (1 + z_{zz}) z_{2p,0}$.²⁹

Although the estimated values of the hole content seem to be reasonable, the dependence of z_{zz} at the Co site against the directly measured v is inconsistent with the results expected from the analyses based on the on-site holes in the CoO₂ layer, because experimental results show that z_{zz} at the Co site increases with decreasing v . If the dependence of z_{zz} were determined by the change of the hole content, z_{zz} should be decreased with decreasing v . In order to understand the change of the z_{zz} at the Co site with respect to v completely, the change of z_{zz} at the O site should be investigated, since the doped hole might be introduced into the O-2p orbitals predominantly. Alternatively, the change of the z_{zz} at the Co site is qualitatively understood by that of V_{lat} as discussed above. It seems that the value of z_{zz} is predominantly determined by the on-site hole contribution, but the change of z_{zz} is by the lattice contribution. We suggest that the observed z_{zz} is not solely determined by the V_{int} , but by the both of V_{lat} and V_{int} .

4.2 Spin Dynamics in cobaltate compounds

As shown in Fig. 5, $1-T_1T$ in the BLH samples indicate a strong sample dependence below 70 K. In this section, we discuss characteristics of the magnetic fluctuations in the BLH compounds. First, $1-T_1T$ in the No. 1 sample ($T_c = 4.7$ K) is compared with that in samples with $T_c = 4.6$ K reported by other groups,^{30,32} which is shown in Fig. 6. It is obvious that $1-T_1T$ in samples with $T_c = 4.6$ K reported so far shows the same behavior in the normal state, indicating that the temperature dependence of $1-T_1T$ in the normal state is intrinsic in the superconducting samples. The possibility is ruled out that the enhancement of $1-T_1T$ in the low-temperature region is due to magnetic fluctuations by impurity moments, since the content of impurity moments would be different in different samples. In the superconducting state, it is clear that $1-T_1$ does not have a coherence peak just below T_c , followed by the T^3 dependence ($1-T_1T \propto T^2$) down to 1 K. This strongly suggests that the superconducting gap has line nodes, resulting in the unconventional

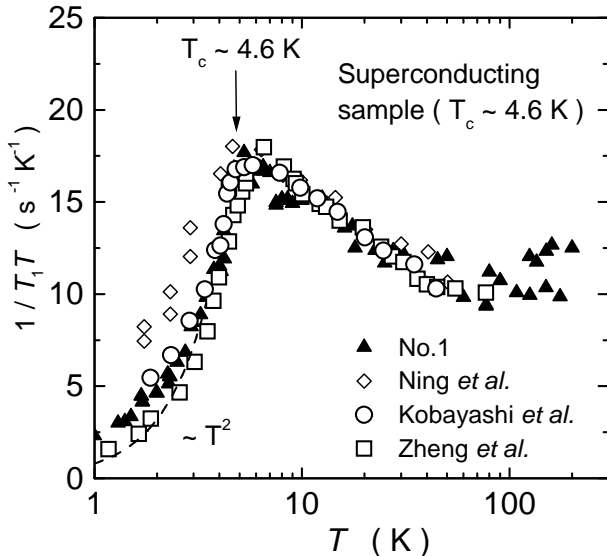


Fig. 6. Temperature dependence of $1/T_1T$ in the superconducting samples with $T_c \sim 4.6$ K reported so far. Temperature dependence of $1/T_1T$ in our No.1 sample ($T_c = 4.7$ K) is compared with that in the superconducting samples with $T_c = 4.6$ K reported by other groups.³⁰⁽³²⁾

superconductivity realized in the BLH cobaltate.^{8,32}

Next, we compare $1/T_1T$ in the superconducting BLH sample (No.1) with $1/T_1T$'s in the non-superconducting MLH sample⁸ and anhydrite $\text{Na}_{0.35}\text{CoO}_2$.³⁰ Figure 7 shows $1/T_1T$ in these samples. $1/T_1T$ in the MLH sample is almost the same as that in the anhydrite sample, both of which show the Korringa behavior in the low temperature region. In contrast, $1/T_1T$ in the superconducting BLH compound is enhanced below 70 K down to T_c , although $1/T_1T$ above 100 K is nearly the same as that in other two samples. It is suggested from the comparison between the BLH and MLH or anhydrite compounds that the low-temperature enhancement of $1/T_1T$ plays an important role for the occurrence of the superconductivity. In the temperature region greater than 100 K, $1/T_1T$ in all samples increases as temperature increases, which is reminiscent of the spin-gap behavior in cuprate superconductors. It is considered that the spin-gap behavior of $1/T_1T$ in the high temperature region is related to the pseudogap revealed by the photoemission experiment.¹⁸ The similar spin-gap behavior was reported in anhydrite Na_xCoO_2 with $x = 0.7$.^{33,34} The spin-gap behavior followed by the $T_1T = \text{const.}$ relation in the MLH and anhydrite samples in Fig. 7 is consistently reproduced by the following function,

$$\frac{1}{T_1T}_{\text{MLH}} = 8.75 + 15 \exp \left(-\frac{T}{T_0} \right) \left(\text{sec}^{-1} \text{K}^{-1} \right)$$

with $T_0 = 250$ K. The value of T_0 is in good agreement with the pseudogap of an energy scale of 20 meV revealed by the photoemission measurement.¹⁸ It seems that the spin-gap behavior is a common feature in cobaltate compounds and would be nothing to do with the superconductivity. Rather, we suggest that the low-temperature enhancement of $1/T_1T$ is decisively related to the superconductivity. The properties of the low-

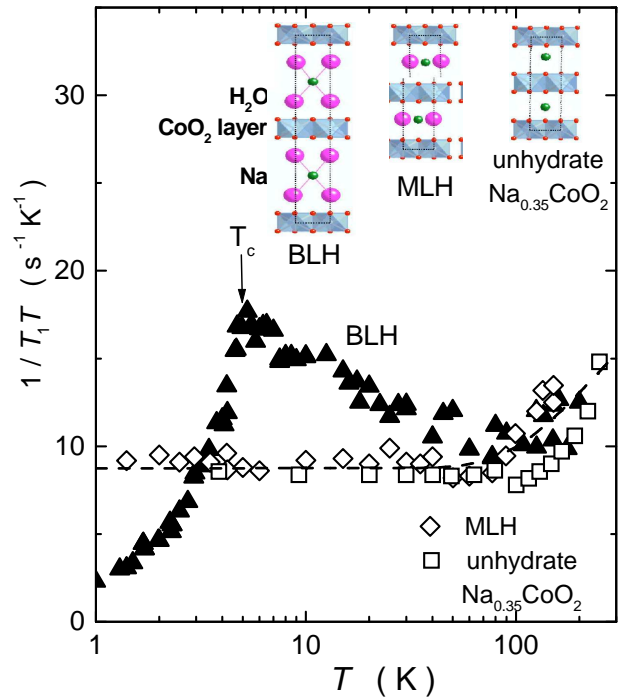


Fig. 7. Temperature dependence of $1/T_1T$ in the superconducting bi-layered hydrate (BLH) sample (No. 1) and monolayered hydrate (MLH) and anhydrite cobaltate $\text{Na}_{0.35}\text{CoO}_2$. The experimental data of the anhydrite cobaltate is referred from Ning et al.³⁰ The dotted line is the fitting curve of $1/T_1T$ in the MLH and anhydrite compounds. (See in text).

temperature spin dynamics are discussed quantitatively.

In order to characterize magnetic fluctuations in the BLH compounds, we analyze the temperature dependence of $1/T_1T$ in the ordered samples at the beginning. Figure 8 shows temperature dependence of $1/T_1T$ in the No. 8 sample, which has the highest NQR frequency and shows the magnetic ordering at $T_M = 6$ K. In the figure, $1/T_1T$ in the MLH compound is also shown. The prominent divergence of $1/T_1T$ is observed at $T_M = 6$ K in the No. 8 sample. We tried to fit the temperature dependence of $1/T_1T$ above T_M by some function, and found that a fairly good fit is obtained by the function consisting of two contributions expressed as,

$$\frac{1}{T_1T}_{\text{No.8}} = \frac{1}{T_1T}_{\text{MLH}} + \frac{20}{T - 6} \left(\text{sec}^{-1} \text{K}^{-1} \right)$$

The former term is the contribution from the spin dynamics originating from the MLH and anhydrite compounds, and the latter is the magnetic contribution, which gives rise to the magnetic ordering. It should be noted that the relation of $1/T_1T / 1 = (T - T_M)$ is the temperature dependence anticipated in the three-dimensional (3-D) itinerant antiferromagnet in the framework of the self-consistent renormalized (SCR) theory.¹⁹ It seems that the relation of $1/T_1T / 1 = (T - T_M)$ for the 2-D antiferromagnet would be more appropriate if the crystal structure of the BLH compound is taken into account, but the experimental data cannot be reproduced by the function of $1/T_1T / 1 = (T - T_M)$ as shown in Fig. 8. From temperature dependence of $1/T_1T$, the or-

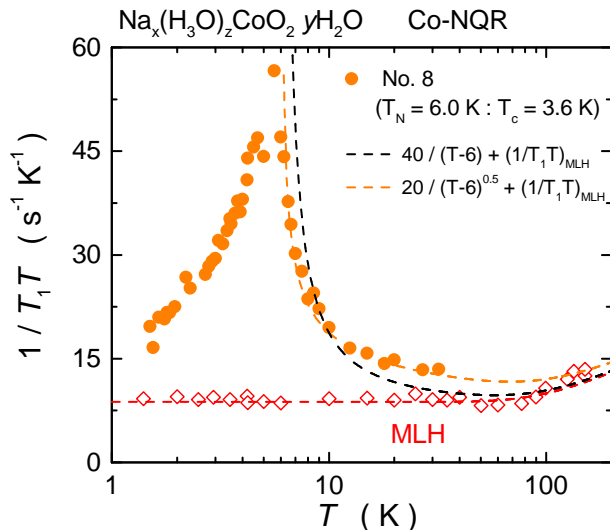


Fig. 8. Temperature dependence of $1/T_1T$ in the No. 8 sample, which shows the magnetic ordering at 6.0 K . $1/T_1T$ in the M-LH compound is also shown. The fitting function for the M-LH compound data is shown by the red dotted line. The orange and black dotted lines are the fitting functions for the No. 8 data above T_M , which are shown in the figure.

dered sample might have the 3-D magnetic correlations just above T_M due to the magnetic ordering even if the dominant fluctuations are 2-D character.

Anyhow, we adopt the fitting function of

$$\frac{1}{T_1T} = \frac{1}{T_1T_{MLH}} + \frac{a}{T}$$

to understand the systematic change of the magnetic fluctuations.

Figure 9 shows the temperature dependence of $1/T_1T$ in No. 5, 7, and 8 samples, together with that in No. 1 and the M-LH compound. The No. 5, 7 and 8 samples have higher frequencies than 12.3 MHz (observed in the No. 1 sample) for the $5=2 \rightarrow 7=2$ transition. As shown in Fig. 9, the systematic change of the temperature dependence of $1/T_1T$ is consistently reproduced by the change of the ordering temperature without changing the coefficient of a .

It should be noted that in the No. 1 sample with $T_c = 4.7\text{ K}$ is evaluated to be $= 1\text{ K}$, which is very close to the quantum critical point of $= 0$. When the superconductivity is suppressed by magnetic fields, it is found that $1/T_1T$ of the sample with $T_c = 4.8\text{ K}$ continues to increase down to 1.5 K . This verifies the validity of the fitting function (not shown here). Detailed experimental results in magnetic fields will be summarized in a separated paper.³⁵

Next, we analyze the temperature dependence of $1/T_1T$ in the superconducting samples using the same fitting function for consistency. Figure 10 shows the temperature dependence of $1/T_1T$ in the superconducting No. 1, No. 3 and No. 11 samples together with the M-LH samples. The temperature dependences of $1/T_1T$ in these samples are satisfactorily fitted by the same function as in the ordered samples using the parameters shown in the figure. It is interesting that the change of the magnetic fluctuations when T_c is increased is understood by

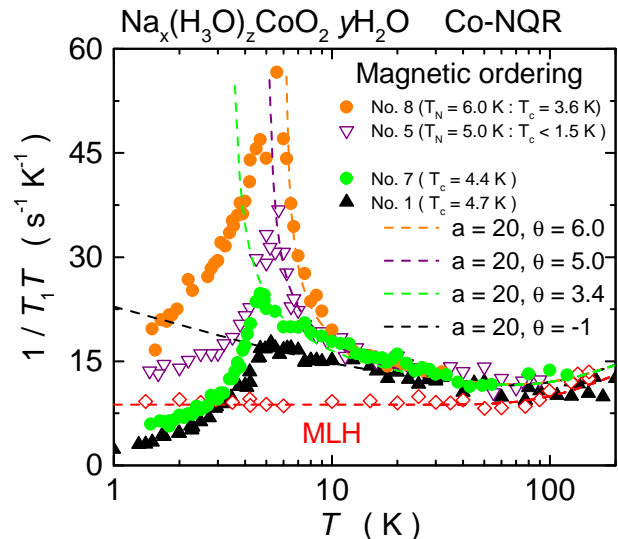


Fig. 9. Temperature dependence of $1/T_1T$ in the magnetically-ordered samples (No. 5 and 8) together with that in the superconducting samples (No. 1 and 7) and the M-LH sample. The dotted lines are the fitting results, and the fitting parameters in each sample are shown in the figure, respectively. (See in the text.)

changing the parameter of a without changing $= 1\text{ K}$ using the same fitting function, which is contrast to the case of the samples showing the magnetic ordering. It is found that the properties of the magnetic fluctuations are systematically understood by the above fittings and that magnetic fluctuations are enhanced with increasing NQR frequencies. It is shown that superconductivity occurs and T_c is increased when the magnetic fluctuations with the quantum critical character appear and are enhanced at low temperatures.

We briefly comment the character of magnetic correlation which is suggested by the NMR and NQR experiments. It is suggested that q -dependence of magnetic fluctuations has a peak in the small q -vector region, since $1/T_1T$ at the O site is scaled to that at the Co site.^{11,30} If there were magnetic correlations with $Q = (;)$, the magnetic correlations at the O site is filtered out due to the symmetric position. In addition, from the temperature dependence of the spin part of the Knight shift which shows gradually increase with decreasing temperature but does not scale to the temperature dependence of $1/T_1T$ below 30 K , it is considered that low-temperature fluctuations developing below 70 K have incommensurate fluctuations with a peak at $q = 0$ other than $q = 0$.¹¹ In the next section, we discuss the relationship between the superconductivity and magnetic fluctuations.

4.3 Relationship between the superconductivity and magnetic fluctuations

As shown in the above section, we show that magnetic fluctuations are sample dependent and seem to be related to the superconductivity. To clarify the relationship between the superconductivity and magnetic fluctuations is very important for understanding the mechanism

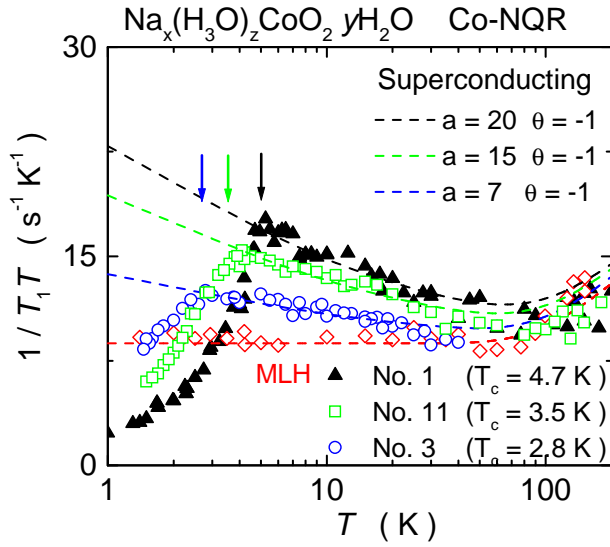


Fig. 10. Temperature dependence of $1/T_1T$ in the various superconducting samples (No. 1, 3 and 11) together with that in the MLH sample. The dotted lines shown in the figure are the fitting results. Fitting parameters in each sample are shown in the figure, respectively. (See in text.)

anism of the superconductivity, because the magnetic fluctuations are considered to suppress s-wave superconductivity, whereas magnetic fluctuations are invoked to give rise to unconventional superconductivity. As shown in Fig. 10, the higher- T_c sample has the stronger magnetic fluctuations. It should be noted that the sample with the stronger magnetic fluctuations shows the sharp decrease of $1/T_1T$ just below T_c . It is considered that the magnitude of SC gap, $2 = k_B T_c$ is larger and the superconductivity therefore is stronger in the sample with stronger magnetic fluctuations. In addition, the sample quality is considered to be nearly equivalent in all BLH samples from the measurement of the FWHM of the NQR spectrum. We consider that these experimental results support the idea that the magnetic fluctuations are the driving force of the superconductivity of the BLH compound. If the magnetic fluctuations were unfavorable for the superconductivity, the decrease of $1/T_1T$ should be moderate just below T_c and the magnitude of $2 = k_B T_c$ should be smaller in the sample with the stronger magnetic fluctuations due to the pair breaking effect by the magnetic fluctuations. It is also noteworthy that the magnetic fluctuations related to the superconductivity are not observed in the MLH compound and the anhydrate $\text{Na}_{0.35}\text{CoO}_2$, but only in BLH compounds. The drastic change in the electronic state is suggested to occur by the further intercalation of water from the MLH structure to the BLH structure. Magnetic fluctuations in the BLH compounds are very sensitive to samples, and the NQR frequencies also show the sample dependence. Next, we show the phase diagram in the BLH compounds using the NQR frequencies, T_c and T_M , and discuss the possible scenario of the superconductivity in the BLH cobaltate.

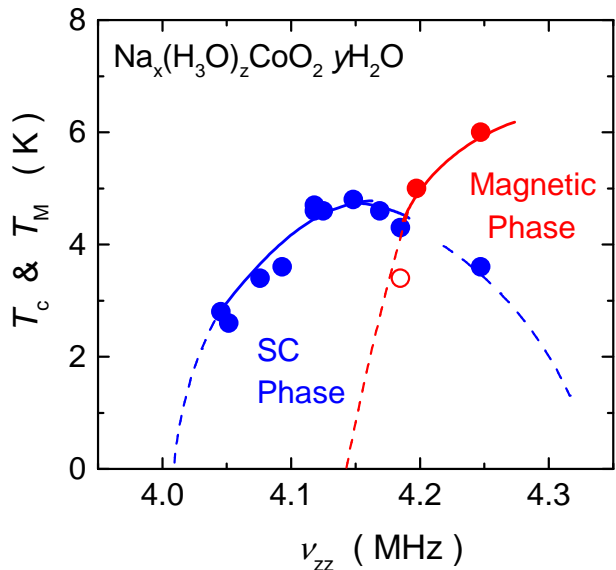


Fig. 11. Phase diagram of $\text{Na}_x(\text{H}_3\text{O})_z\text{CoO}_2-y\text{H}_2\text{O}$, in which z is treated as a tuning parameter. The sample with the highest z shows a magnetic anomaly at 6 K and superconductivity at 3.5 K. The fitting result for the No. 7 sample is also shown by the red circle.

4.4 Phase diagram of the BLH compounds and the possible scenario of the superconductivity

As shown and discussed above, it was found that the NQR frequency of the Co site is very sensitive to samples, which seems to detect the important change of the Co electronic state. In the previous paper, we plotted T_c against the NQR frequencies arising from the $5=2 \rightarrow 7=2$ transition and developed the possible phase diagram in $\text{Na}_x(\text{H}_3\text{O})_z\text{CoO}_2-y\text{H}_2\text{O}$.⁹

Figure 11 shows the new phase diagram using the experimental data of twelve samples, where the horizontal axis is changed to z . It is found that the superconducting phase shows the " dome " behavior against z , and that the highest T_c is observed at the point where T_M becomes zero, i.e. at the quantum critical point. The phase diagram we develop is reminiscent of that in the Ce-based heavy-fermion superconductors, where antiferromagnets change to superconductors by pressure application.^{36,37} We consider that the superconductivity of the BLH cobaltate is induced by the quantum critical fluctuations as suggested in the heavy-fermion superconductivity.³⁶

It is shown that the occurrence of the superconductivity is highly sensitive to the z and c -axis parameter. We discuss the physical meaning of the horizontal axis of the phase diagram in the BLH-cobaltate superconductor. We consider that the change of z is mainly due to the change of V_{lat} , which is related to the CoO_2 block layer thickness. The crystal distortion along the c axis splits t_{2g} levels of Co-3d orbitals into doublet e_g^0 states and singlet a_{1g} state. Therefore, z is regarded as the physical parameter related to the crystal-field splitting between a_{1g} and e_g^0 . According to a band calculation, these two different orbitals cross the Fermi energy and form two kinds of Fermi surfaces (FS); six hole pockets

around K points (e_g^0 -FS) and a large hole Fermi surface around a_{1g} point (a_{1g} -FS).¹⁵ When e_g^0 levels are lifted and reach Fermi energy to form e_g^0 FS's by the crystal distortion and the further crystal field splitting, it is considered that the hole-character e_g^0 FS's appear and increase the volume.

We point out that the above scenario consistently explain the change of the magnetic fluctuations from the anhydrate $\text{Na}_{0.35}\text{CoO}_2$ and the MLH compound to the BLH compound. As shown in Fig. 7, the temperature dependence of $1=T_1T$ in the anhydrate and MLH compounds are nearly the same, which are determined by the a_{1g} -FS. The Korringa behavior and the pseudogap behavior are also suggested theoretically from the properties of the magnetic fluctuations originating from the a_{1g} -FS.²² Low-temperature behavior of $1=T_1T$ in the BLH compounds, which is expressed as $a = \frac{1}{T}$, is considered to originate from the e_g^0 -FS's. We point out that the magnetic fluctuations in the BLH compounds are consistently interpreted by the multiband properties because two different temperature dependence is observed in $1=T_1T$. In addition, we found that $1=T_1T$ in the samples with lower T_c and lower z_2 shows a weaker temperature dependence and $1=T_1T$ in the samples with higher T_c and higher z_2 becomes enhanced below 70 K. Temperature dependence of $1=T_1T$ indicates that the magnetic fluctuations around T_c are enhanced with increasing z_2 . We consider that the development of magnetic fluctuations around T_c is consistently understood by the change of the volume of the e_g^0 -FS by the small crystal distortions along the c axis.

These experimental results we show here seem to be consistently understood by the theoretical scenario developed by Mochizuki et al., in which the magnetic fluctuations with the small characteristic wave vector q are induced by the nesting of the e_g^0 -FS.²⁰ Although ferromagnetic fluctuations with the peak at $q = 0$ were excluded from the comparison between bulk and $1=T_1T$ in the superconducting compounds, the magnetic fluctuations with $q \neq 0$ seem to be consistent with the experimental result. Detailed inelastic neutron-scattering measurements are needed to reveal the character of the magnetic fluctuations in the superconducting samples. In addition, the detailed ARPES experiment on the superconducting $\text{Na}_x(\text{H}_3\text{O})_z\text{CoO}_2 \cdot y\text{H}_2\text{O}$ is also desired, although the absence of the e_g^0 -FS was reported on the anhydrate $\text{Na}_{0.35}\text{CoO}_2$. It is suggested from the $1=T_1T$ results shown in Fig. 7 that the FS's on the anhydrate and MLH compounds are quite different from those on the BLH compounds.

4.5 Coexistence of Magnetism and Superconductivity

In the No. 5 and 8 samples, we found the magnetic ordering at T_M . Detailed results on the No. 5 sample were already published in the previous paper.⁹ Here we show the coexisting phenomenon of superconductivity and magnetism observed in the No. 8 sample. As shown in Fig. 5, we found the prominent peak in $1=T_1T$ in No. 8 at 6 K, below which the internal field appears at the Co site. Figure 12 shows the Co-NQR spectra above and below T_M . Three well-separated peaks above T_M be-

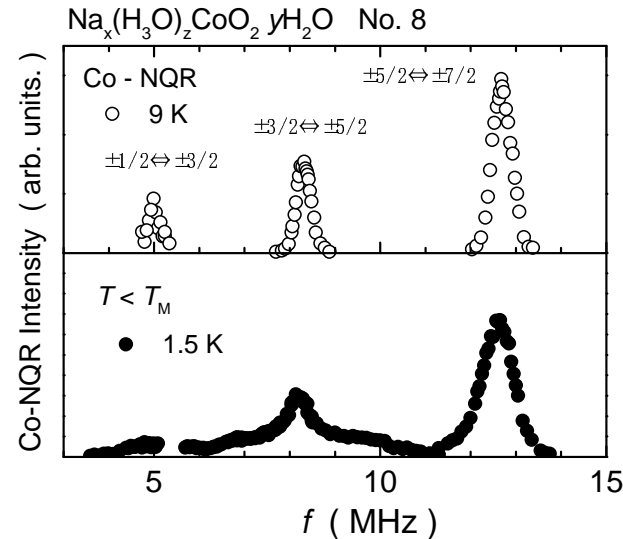


Fig. 12. Co-NQR spectra in the No. 8 sample. Upper figure is the spectrum at 9 K above T_M , and the lower figure is at 1.5 K below T_M .

come broad below T_M due to the internal field at the Co-nuclear site, which originates from the Co-3d spins and is mediated by the hyperfine coupling between Co-3d spin and Co-nuclear moment. From the structureless spectrum below T_M , the magnitude of the internal field is considered to be distributed.

When the Co nuclear spins with the electric quadrupole interaction are in the magnetic field, the Zeeman interaction is added to the total nuclear Hamiltonian. The Zeeman interaction is expressed as

$$H_Z = n \sim I \cdot H_{\text{int}}$$

, where n and H_{int} are the Co nuclear gyromagnetic ratio and internal field at the Co site, respectively. The structureless broad spectrum is approximately reproduced by using the inhomogeneous internal field in the CoO_2 plane as shown in the inset of Fig. 13. Here, the magnitude of the internal field is distributed, suggestive of the inhomogeneous ordered moments lying in the CoO_2 plane.

Below 3.5 K, the Meissner shielding was observed. Superconducting transition of No. 8 is broader, but the magnitude of the Meissner shielding is comparable to that in other samples as shown in Fig. 14. From the temperature dependence of $1=T_1T$ measured at 12.69 MHz, the clear anomaly associated with the superconducting transition was not detected in the temperature dependence of $1=T_1T$. The recovery of the nuclear magnetization after the saturation pulses is consistently fitted by the single component of T_1 . We also measured $1=T_1T$ at various frequencies around 8.5 MHz, where the internal field is distributed from zero to 1 kOe as shown in Fig. 13. The values of $1=T_1T$ at 1.5 K are nearly the same over these frequencies. These experimental results rule out the macroscopic phase separation between superconducting and magnetic regions, but suggest microscopic coexistence between superconductivity and magnetism. We point out that the similar coexistence is observed in

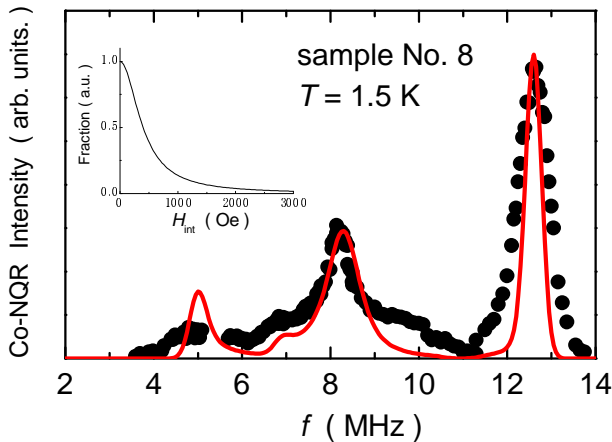


Fig. 13. Simulation of the NQR spectrum at 1.5 K. The red line is the calculation of the NQR spectrum using the inhomogeneous internal field shown in the inset.

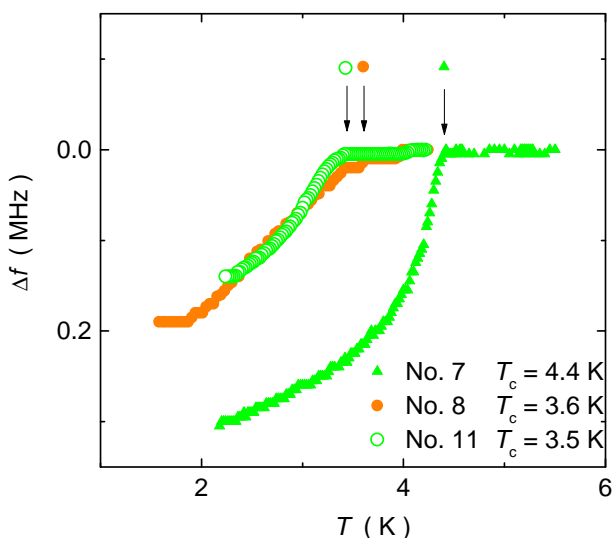


Fig. 14. The ac susceptibility measurements on the No. 7, 8, and 11 samples using the in-situ NQR coil. The superconducting transition on No. 8 is broad, but the Meissner signal of No. 8 is comparable to that on No. 11, which has a similar T_c .

the slightly Ge-doped CeCu_2Si_2 ³⁸ and CeRhIn_5 under 1.6 GPa,³⁹ which are located in the vicinity of the border between superconductivity and magnetism in the Ce-based heavy-fermion superconductors. We suggest that such inhomogeneous coexistence is characteristics of the coexisting compounds with T_M being higher than T_c . In order to investigate the relationship between superconductivity and magnetism in $\text{Na}_x(\text{H}_3\text{O})_z\text{CoO}_2 \cdot y\text{H}_2\text{O}$, further experiment is still needed, particularly pressure experiments on the No. 8 sample are considered to be very important.

5. Conclusion

We performed Co-NQR measurements on various samples with different values of T_c and T_M . We found that the nuclear quadrupole frequency q strongly depends on the samples. We show that the asymmetric parameter is almost unchanged (~ 0.2) in these samples, and

suggests that the presence of the holes in both a_{1g} and e_g^0 orbitals is important for understanding the nature, although the ordering of Na and oxonium ions in the Na-hydrate block layer should be taken into account. In contrast to the unchanged q , the electric field gradient zz depends on the samples and has a linear relation with the c -axis parameter. We consider that the sample dependence of zz originates mainly from the trigonal distortion of the CoO_2 layer, which splits the t_{2g} levels of Co 3d orbital into e_g^0 and a_{1g} levels. We also show that the magnetic fluctuations, which develop below 70 K, is one of the characteristic features observed in the BLH compounds, and that the fluctuations are strongly related with the occurrence of the superconductivity. We found that the magnetic fluctuations are also related to the zz , and suggest that zz is one of the most important physical parameters to characterize the sample properties of superconducting and non-superconducting $\text{Na}_x(\text{H}_3\text{O})_z\text{CoO}_x \cdot y\text{H}_2\text{O}$ compounds. We develop the phase diagram using the experimental results on the twelve samples, and show that the high- T_c sample is situated near the point where T_M becomes zero. The microscopic coexistence of the superconductivity and magnetism is suggested in the No. 8 sample, which is also similar to that in the Ce-based superconductors. We conclude that the BLH cobaltate is an unconventional superconductor induced by the quantum critical fluctuations, which shares a lot of common aspects with the Ce-based heavy-fermion superconductors.

Acknowledgments

We thank Y. Iitho, H. Ohta, H. Yaguchi, S. Nakatsuji and Y. Maeno for experimental support and valuable discussions. We also thank S. Fujimoto, K. Yamada, Y. Yanase, M. Mochizuki, and M. Ogata for valuable discussions. This work was partially supported by CREST of the Japan Science and Technology Agency (JST) and the 21 COE program on "Center for Diversity and Universality in Physics" from MEXT of Japan, and by Grants-in-Aid for Scientific Research from the Japan Society for the Promotion of Science (JSPS) (No. 16340111 and 18340102) and MEXT (No. 16076209).

- 1) K. Takada, H. Sakurai, E. Takayama-Muromachi, F. Izumi, R. A. Dilanian, and T. Sasaki: *Nature* **422** (2003) 53.
- 2) J. D. Ferguson, M. A. Vdovin, D. G. Hinks, J. C. Burley, and S. Short: *Phys. Rev. B* **68** (2003) 214517.
- 3) M. L. Foo, R. E. Schaak, V. L. Miller, T. Klimczuk, N. S. Rogado, Y. Wang, G. C. Lau, C. C. Raley, H. W. Zandbergen, N. P. Ong, and R. J. Cave: *Solid State Commun.* **127**, 33 (2003).
- 4) K. Takada, H. Sakurai, E. Takayama-Muromachi, F. Izumi, R. A. Dilanian, and T. Sasaki: *J. Solid. State. Chem.* **177** (2004) 372.
- 5) R. Arita: *Phys. Rev. B* **71** (2005) 132503.
- 6) B. P. Bayrakci, I. Mirebeau, P. Bourges, Y. Sidis, M. Enderle, J. Mesot, D. P. Chen, C. T. Lin, and B. Keimer: *Phys. Rev. Lett.* **94** (2005) 157205.
- 7) L. M. Helm, A. T. Boothroyd, R. C. Oldea, D. P. Rabrahakaran, D. A. Tennant, A. Hiess, and J. Kulda: *Phys. Rev. Lett.* **94** (2005) 157206.
- 8) K. Ishida, Y. Ihara, Y. Maeno, C. Mochioka, M. Kato, K. Yoshimura, K. Takada, T. Sasaki, H. Sakurai, and

E. Takayama-Muroguchi: *J. Phys. Soc. Jpn.* 72 (2003) 3041.

9) Y. Ihara, K. Ishida, C. M. Ichioka, M. Kato, K. Yoshimura, K. Takada, T. Sasaki, H. Sakurai, and E. Takayama-Muroguchi: *J. Phys. Soc. Jpn.* 74 (2005) 867.

10) Y. Ihara, K. Ishida, C. M. Ichioka, M. Kato, K. Yoshimura, K. Takada, T. Sasaki, H. Sakurai, and E. Takayama-Muroguchi: *J. Phys. Soc. Jpn.* 73 (2004) 2069.

11) Y. Ihara, K. Ishida, K. Yoshimura, K. Takada, T. Sasaki, H. Sakurai and E. Takayama-Muroguchi: *J. Phys. Soc. Jpn.* 74 (2005) 2177.

12) Y. Ihara, K. Ishida, H. Takeya, C. M. Ichioka, M. Kato, Y. Itoh, K. Yoshimura, K. Takada, T. Sasaki, H. Sakurai and E. Takayama-Muroguchi: *J. Phys. Soc. Jpn.* 74 (2006) 2177.

13) J. W. Lynn, Q. Huang, C. M. Brown, V. L. Miller, M. L. Foo, R. E. Schaak, C. Y. Jones, E. A. Mackey, and R. J. Cava: *Phys. Rev. B* 68 (2003) 214516.

14) H. Sakurai, K. Takada, T. Sasaki and E. Takayama-Muroguchi: *J. Phys. Soc. Jpn.* 74 (2005) 2909.

15) D. J. Singh: *Phys. Rev. B* 61 (2000) 13397.

16) D. Qian, L. Wray, D. Hsieh, D. Wu, J. L. Luo, N. L. Wang, A. Kuprin, A. Fedrov, R. J. Cava, L. Viciu and M. Z. Hasan: *Phys. Rev. Lett.* 96 (2006) 046407.

17) H.-B. Yang, Z.-H. Pan, A. K. P. Sekharan, T. Sato, S. Souma, T. Takahashi, R. Jin, B. C. Sales, D. M. Andrus, A. V. Fedrov, Z. Wang and H. Ding: *Phys. Rev. Lett.* 95 (2005) 146401.

18) T. Shimojima, T. Yokoya, T. Kiss, A. Chainani, S. Shin, T. Togashi, C. Zhang, C. Chen, S. Watanabe, K. Takada, T. Sasaki, H. Sakurai and E. Takayama-Muroguchi: *J. Phys. Chem. Solids*, 67 (2006) 282.

19) T. Mori et al.: *J. Mag. Mag. Mat.* 100 (1991) 261.

20) M. Mochizuki, Y. Yanase, and M. Ogata: *J. Phys. Soc. Jpn.* 74 (2005) 1670.

21) Y. Yanase, M. Mochizuki, and M. Ogata: *J. Phys. Soc. Jpn.* 74 (2005) 2568.

22) K. Yada and H. Kontani: *J. Phys. Soc. Jpn.* 74 (2005) 2161.

23) C. J. Mihel, D. N. Argyriou, A. Chemtadine, N. A. Liouane, J. Veira, S. Landsgesell, and D. Alber: *Phys. Rev. Lett.* 93 (2004) 247007.

24) K. Takada, K. Fukuda, M. Osada, I. Nakai, F. Izumi, R. A. Didurian, K. Kato, M. Takata, H. Sakurai, E. Takayama-Muroguchi and T. Sasaki: *J. Mat. Chem.* 14 (2004) 1448.

25) G.-q. Zheng, K. Matano, R. L. Meng, J. Cmaidala and C. W. Chu: *cont-mat/0601089*.

26) K. Hanazawa, F. Komatsu and K. Yosida: *J. Phys. Soc. Jpn.* 59 (1990) 3345.

27) R. Ray, A. G. Hoshnay, K. G. Hoshnay and S. Nakamura, *Phys. Rev. B* 59 (1999) 9454.

28) I. Mukhammedshin, H. Aloul, G. Collin, and N. Blanchard: *Phys. Rev. Lett.* 94 (2005) 247602.

29) G.-q. Zheng, Y. Kitao, K. Ishida and K. Asayama: *JP SJ* 64, 2524 (1995).

30) F. Ling and T. Imai: *Phys. Rev. Lett.* 94 (2005) 188301.

31) Y. Kobayashi, H. Watanabe, M. Yokoi, T. Miyoshi, Y. Mori and M. Sato: *J. Phys. Soc. Jpn.* 74 (2005) 1800.

32) T. Fujimoto, G.-q. Zheng, Y. Kitao, R. L. Meng, J. Cmaidala and C. W. Chu: *Phys. Rev. Lett.* 92 (2004) 047004.

33) F. Ling, T. Imai, B. W. Statt and F. C. Chou: *Phys. Rev. Lett.* 93 (2004) 237201.

34) M. Yokoi, T. Miyoshi, Y. Kobayashi, M. Soda, Y. Yasui, M. Sato and K. Kurokura: *J. Phys. Soc. Jpn.* 74 (2005) 3046.

35) Y. Ihara, to be published.

36) N. D. Mathur, F. M. G. Roshe, S. R. Julian, I. R. Walker, D. M. Freye, R. K. M. Haselwimmer and G. G. Lonzarich: *Nature* 394 (1998) 39.

37) S. Kawasaki, T. Mito, G.-q. Zheng, C. Hessieu, Y. Kawasaki, K. Ishida, Y. Kitao, T. Muraatsu, T. C. K. Kobayashi, D. Aoki, Y. Haga, R. Settai and Y. Onuki: *Phys. Rev. B* 65 (2004) 20504.

38) Y. Kawasaki, K. Ishida, K. Obinata, K. Tabuchi, K. Kashima, Y. Kitao, O. Trovarelli, C. G. Eibel, and F. Steglich: *Phys. Rev. B* 66 (2002) 224502.

39) T. Mito, S. Kawasaki, Y. Kawasaki, G.-q. Zheng, Y. Kitao, D. Aoki, Y. Haga and Y. Onuki: *Phys. Rev. Lett.* 90 (2003) 077004.

40) Y. Ihara, H. Takeya, K. Ishida, C. M. Ichioka, K. Yoshimura, K. Takada, T. Sasaki, H. Sakurai and E. Takayama-Muroguchi: appear in *AP*.